LUPINE PUBLISHERS

ISSN: 2641-6921

Modern Approaches on Material Science

DOI: 10.32474/MAMS.2021.05.000201

Review Article

Structural Analysis of Nanoparticle Zirconium Dioxide: A Comprehensive Review

Gunel T Imanova[1]* and Mustafa Kaya[2]

[1]*Department of Physical, Mathematical and Technical Sciences, Institute of Radiation Problems, Azerbaijan National Academy of Sciences, Azerbaijan*

[2]*Department of Chemical Engineering, Siirt University, Siirt, 56100, Turkey*

***Corresponding author:** Gunel T Imanova, Department of Physical, Mathematical and Technical Sciences, Institute of Radiation Problems, Azerbaijan National Academy of Sciences, AZ 1143 - Baku, Azerbaijan

Received: November 6, 2021 **Published:** November 29, 2021

Abstract

The X-ray diffraction spectrum of the nano-ZrO_2 compound was drawn by the Ritveld method and the crystal structure was determined at room temperature and under normal conditions. The pure zirconia has three different crystal structures: monoclinic, m-ZrO_2, tetragonal, t-ZrO_2, and cubic, c-ZrO_2. The main purpose of writing this review article is: on the surface of nanoparticles of zirconium dioxide, to convey to new researchers the results I have obtained and the results obtained by researchers around the world.

Keywords: Nanoparticle zirconium dioxide; Monoclinic; Tetragonal; Cubic

Crystal Structure Of Nano-Zro_2 (References From Articles Of World Scientists)

The pure zirconia has three different crystal structures: monoclinic, m-ZrO_2, tetragonal, t-ZrO_2, and cubic, c-ZrO_2 [1]. The crystal structures are shown in (Figure 1) At room temperature, ZrO2 is in a monoclinic phase. The phase transition from m-ZrO_2 to t-ZrO_2 takes place at about 1,447 K. Above 2,650 K, the t-ZrO_2 transforms to c-ZrO_2, which is stable up to the melting point at 2,950 K. The c-ZrO2 has an ideal fluorite structure (shown in (Figure 1a). The Zr cations are situated in a face-centered cubic (fcc) lattice, i.e. at the corners of the cubic elementary cell as well as at the halves of the [110] directions. The oxygen anions lie at the quarters of [111] directions, which are the tetrahedral interstitial sites associated with this fcc lattice. The space group is O5 h or Fm3 m. In this structure, each Zr cation is coordinated to eight equivalent nearest-neighbor oxygen anions at the corners of a cube, and each O anions is tetrahedrally coordinated to four Zr cations [1]. Consequently, zirconium and oxygen are octahedrally and tetrahedrally coordinated, respectively. The unite cell contains one zirconium and two oxygen atoms with Zr–O distances of *2.2 A° [1]. The t-ZrO_2 represents a slightly distorted cubic structure (shown in (Figure 1b), obtained by displacing opposite pairs of oxygen atoms alternatively up and down along the [001] direction. In the tetragonal ZrO_2, each Zr cation is still surrounded by eight oxygen anions, with four oxygen neighbors arranged in a flattened tetrahedron at a short Zr–O distance, 2.065 A°, and the rest in an elongated tetrahedron rotated 90 at a distance of 2.455 A° from Zr. Each oxygen anion is bonded to two Zr cations at 2.065 A° , and two more Zr cations are 2.455 A° away. The space group is D15 4h or P42/nmc [1]. The m-ZrO2 has a lower symmetry and a more complex geometric structure, and the primitive cell contains 4 ZrO2, namely 12 atoms (shown in (Figure 1c). Stabilized zirconia has unique physicochemical, mechanical and electrical properties which make it an extraordinary ceramic material of huge interest for a wide variety of applications and industries.

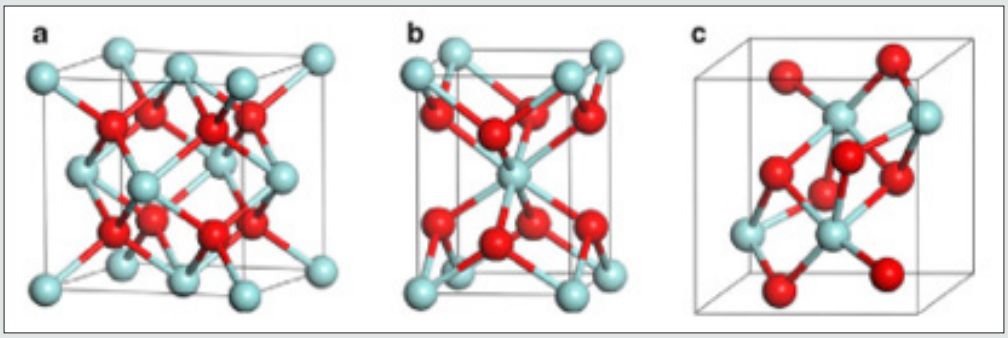

Figure 1: Crystal structures of ZrO_2: a cubic, b tetragonal, and c monoclinic. Red and blue spheres correspond to oxygen and zirconium atoms, respectively.

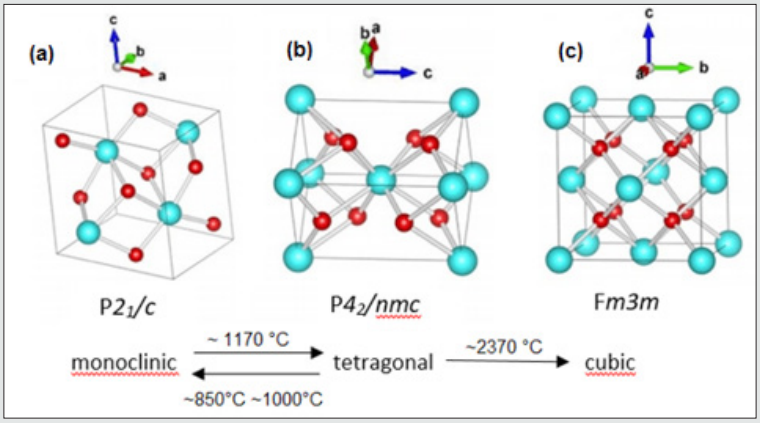

Figure 2: Zirconia phase transformations. As temperature increases, zirconia transforms from monoclinic (a), to tetragonal (b) to cubic (c)[2].

Pure zirconia can exist in one of three states depending on the temperature [2] (Figure 2). Zirconia exists in its monoclinic phase at room temperature, but at temperatures higher than 1,175 °C it transforms to a tetragonal phase. The transformation corresponds to altered characteristics that provide high component and flexural strength, exceptional wear resistance, and excellent durability. These highly desirable properties mean the tetragonal phase has a number of useful applications and it is often employed for structural ceramics in physically demanding applications. If the temperature rises beyond 2,370 °C, zirconia transforms into its cubic state. (Figure 3(a)) shows the refined crystal structure of the tetragonal phase [3]. The axial ratio c/aF was 1.0186, which is a little smaller than that (1.0204) obtained by the extrapolation of the c/aF values of metastable bulk tetragonal zirconia solid solutions. Here aF denotes the lattice parameter based on the pseudo-fluorite lattice, i.e. aF ¼ 21=2 a, where a is the lattice parameter of the tetragonal phase. The fractional z coordinate of the O atom in the tetragonal phase was refined to be 0.2041 (2), which is a little larger than that obtained for bulk tetragonal zirconia at high temperatures. These differences could be ascribed to a nano-sized effect. The displacement of the O atom along the c axis of 0.237 (1) A˚ was confirmed, leading to two different values of the bond lengths between the cation and the anion [R = 2.3562 (6) A˚ and r = 2.0805 (5) A˚ in (Figure 3a)]. The unit-cell volume of the monoclinic phase was larger than that of the tetragonal phase. This is also the case in the bulk zirconia and its solid solutions. The occupancy factor of the O atom in the tetragonal phase was refined to be 0.984 (4). This suggests that the tetragonal ZrO_2 has an oxygen deficiency [R = 0.031 (7)]. The corresponding chemical formula of the tetragonal phase was ZrO_2 [R= 0.031 (7)]. On the contrary, the monoclinic phase did not have an oxygen deficiency within experimental error. These results suggest that the phase transition from monoclinic totetragonal in zirconium oxide nanocrystallites could be caused by the oxygen deficiency as is the tetragonal to cubic transition in the nanocrystallites. Similar behavior has been reported in the tetragonal–cubic phase boundary in bulk crystals of stabilized zirconia: the tetragonal–cubic phase boundary decreases with increasing oxygen defect concentration. The MEM electron-density map shown in (Figure 3(b)) is consistent with the refined crystal structure of the tetragonal phase. The electrons are located at the positions of the Zr and O atoms. No extra peaks are observed in the MEM electron-density map. The MEM density map also suggests the anisotropic distribution of the cation, which could be ascribed to the thermal motion or static disorder. Larger and smaller distributions

of electrons exist around the cation along the longer and shorter Zr—O bonds, respectively (Figure 3b). The MEM density map in Fig. 3(c) indicates covalent bonding between Zr and O atoms. The bond with the shorter Zr—O length, r, has stronger bonding, while the bond with the longer distance, R, has weaker bonding [3].

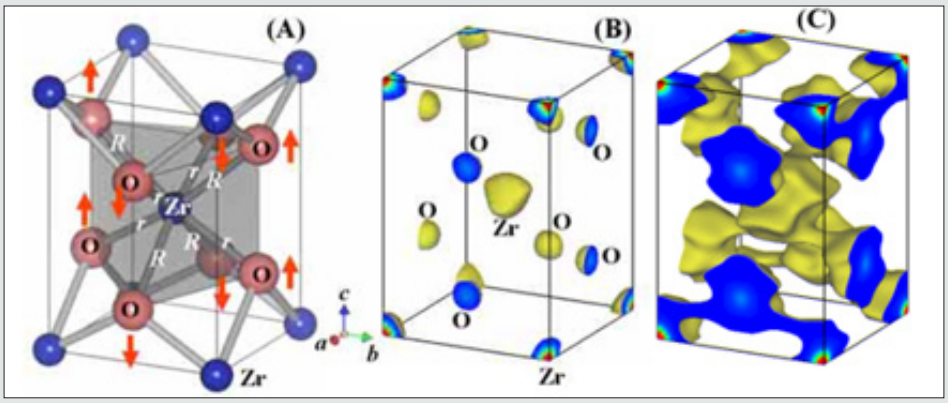

Figure 3: Refined crystal structure (a) and equi-electron-density surfaces at 10 (b) and 1 A˚ 3 (c) of the tetragonal zirconium oxide nanoparticles. The two bond lengths between the cation and anion are R=2.3562 (6) and r=2.0805 (5) A˚. The arrows represent the displacements of the O atoms along the c axis [0.237 (1) A˚]

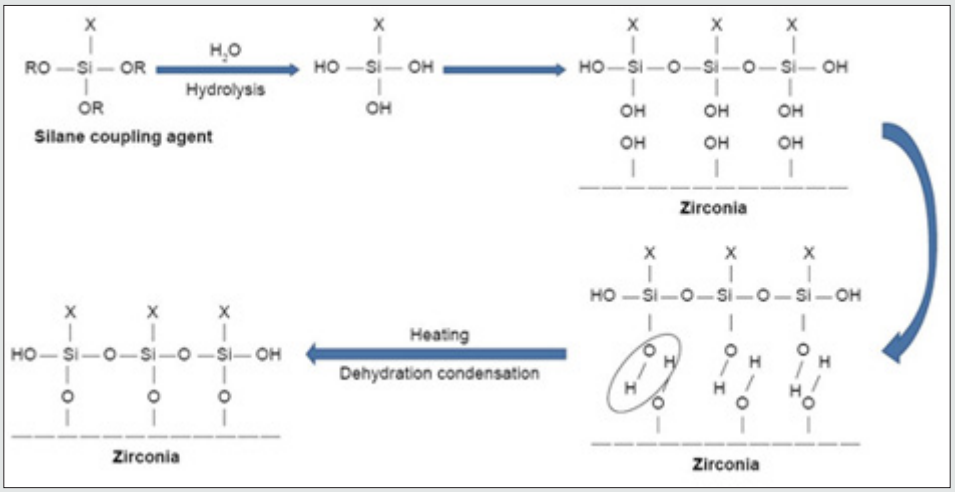

Figure 4: Schematic diagram of silanization of nano-ZrO_2.

Then, (Figure 4) required amount of the solution was placed in a 50-mL bottle, and appropriate amount of Zirconium n-propoxide was added to it, followed by 1 h stirring at RT. In this work, the water/Zr-propoxide molar ratio was kept as 1:4. Based of that, the required amount of an equimolar mixture of n-propanol and water was added to the solution (each film need 0.153 g). This was followed by overnight stirring at RT to promote the sol-gel processing [4]. The resulting mixture was, then, cast in Teflon Petri dish and, because of solvent elution, thin film was obtained. Both types of film (CS-ZrOx and PVA-ZrOx) with the same amount of zirconia (10 wt %) in the polymer matrix were dried at 50 °C for 18 h and, then, left under vacuum for 48 h at the same temperature, for complete removal of solvent. Eventually, flexible hybrid films yielded were calcined at the temperatures, and for the time durations, above specified. The produced zirconia nanopowders were sieved through a 63 μm mesh size, and kept dry till further use. The TMSPM silane coupling agent (Shanghai Richem International Co., Ltd., Shanghai, China) was added to the nano-ZrO_2 particles to coat the surface and form reactive groups, thus allowing for interaction between the resin matrix and nanoparticles and eventual bonding [4]. The process of coating involved dissolving 0.3 g of TMSPM in 100 mL of acetone followed by adding 30 g of nano-ZrO_2 to the TMSPM/acetone mix and stirring for 60 min with a magnetic stirrer (Cimarec Digital Stirring Hotplates, SP131320-33Q; Thermo Fisher Scientific, Waltham, MA, USA). The mixture was placed under vacuum at 60°C in a rotary evaporator at 150 rpm for 30 min to eliminate the acetone. The sample was then heated at 120°C for 2 h to increase the interaction between nano-ZrO_2 and TMSPM and subsequently coupling reaction to occur,[4] and then cooled to obtain silanized nano-ZrO_2. TMSPM can couple the nano-

ZrO_2 PMMA. (Figure 4). shows the schematic representation of the chemical reaction of silanization process, the bonding formed between the nano-ZrO_2 and TMSPM that mainly depends on the functional groups of TMSPM. After hydrolysis of TMSPM, silanol is formed, and alkoxy group is replaced by hydroxyl group (Si–OH) that reacts with hydroxyl group of zirconia (Zr–OH) followed by dehydration condensation reaction resulting in the formation of chemical bonds between nano-ZrO_2 and TMSPM (Zr–O–Si). On the other hand, organofunctional groups (X) contain double bond (C=C) that can bond to PMMA.

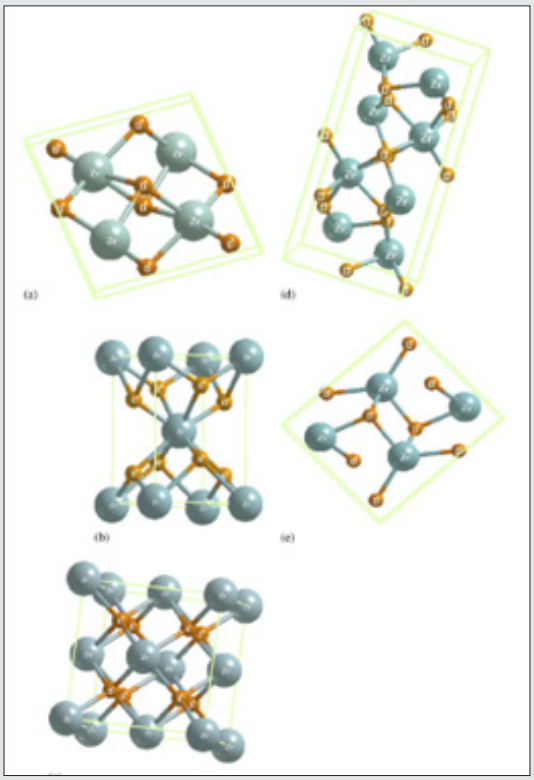

Figure 5: Crystal structures of zirconia polymorphs: (a) monoclinic, (b)tetragonal, (c) cubic, (d) brookite and (e) cotunnite.

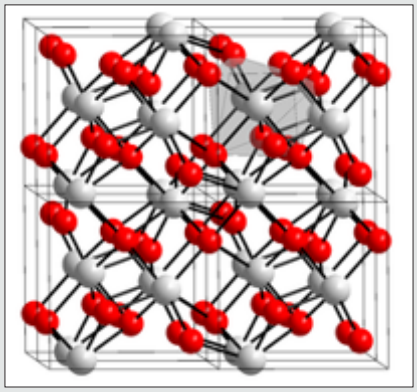

Figure 6: Structure zirconium dioxide.

Zirconia is known to have three low-pressure structural phases (see Figure 5); at low temperature, the monoclinic phase (space group C5 2h or P21/c) is stable [5]. Around 1400 K, there is a first-order displacive martensitic phase transition to a tetragonal structure (space group D15 4h or P42/nmc). The only internal structural parameter of the tetragonal phase is the parameter z of the oxygen position 4d (0, 1 2, z) [5]. At a temperature of about 2600 K, the tetragonal phase transforms into the cubic fluorite structure (space group O5 h or Fm3m), which in turn melts at 2950 K. This phase is a special case of tetragonal structure and can be obtained from the latter by making the ratio of the lattice constants c/a equal to 2 p and by shifting pairs of oxygen atoms in the z direction to their central positions in the unit cell. Zirconium dioxide (ZrO_2), (Figure 6) sometimes known as zirconia (not to be

confused with zircon), is a white crystalline oxide of zirconium. Its most naturally occurring form, with a monoclinic crystalline structure, is the mineral baddeleyite. A dopant stabilized cubic structured zirconia, cubic zirconia, is synthesized in various colours for use as a gemstone and a diamond simulant. hree phases are known: monoclinic below 1170 °C, tetragonal between 1170 °C and 2370 °C, and cubic above 2370 °C. The trend is for higher symmetry at higher temperatures, as is usually the case. A small percentage of the oxides of calcium or yttrium stabilize in the cubic phase. The very rare mineral tazheranite, $(Zr,Ti,Ca)O_2$, is cubic [6]. Zirconium oxide (ZrO_2) is a refractory material and is also known as zirconia or baddeleyite that is a rare zirconium oxide mineral. It has three solid phases (monoclinic, tetragonal and cubic crystals) as shown in (Figure 7a). It changes from monoclinic to tetragonal at 1400 K and to cubic at 2641 K as shown in (Figure 7b). The cubic phase has a fluorite crystal structure. The monoclinic-to-tetragonal change is accompanied by a large volume reduction of ~7.5%, resulting in significant stresses. (Figure 7c) indicates that dense parts may be obtained by sintering of the cubic or tetragonal phase only [7,8] (Figure 8).

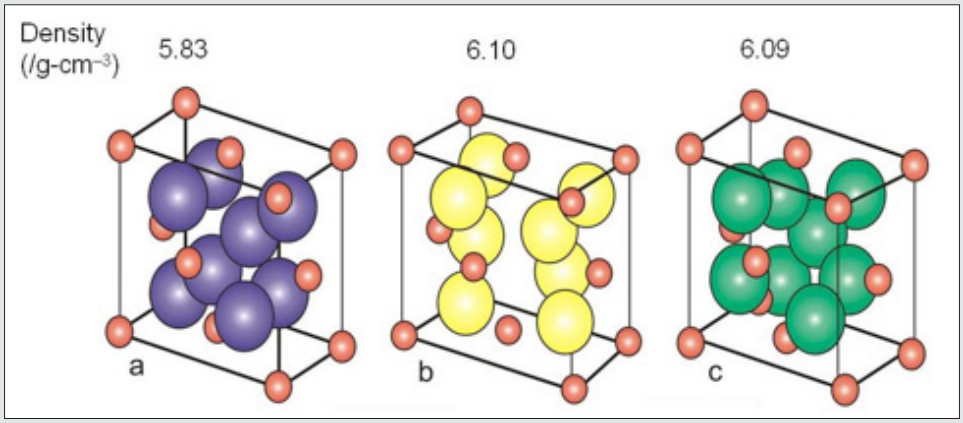

Figure 7: Crystal structure of monoclic (a), tetragonal (b) and cubic zirconia(c). Red spheres represent O atoms, while the other colors represent Zr atoms.

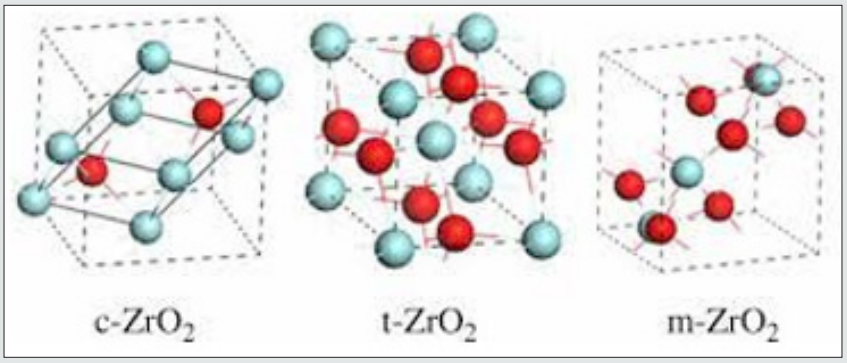

Figure 8: Crystal structure of monoclic (a), tetragonal (b) and cubic zirconia(c). Red spheres represent O atoms, while the other colors represent Zr atoms.

X-Ray Analysis Of Nano Zro_2 (References From Articles Of My And World Scientists)

(Figure 9) shows the X-ray diffraction spectrum of the nano-ZrO2 compound at room temperature and normal conditions. Analysis of the X-ray diffraction spectrum by the Ritveld method revealed that the crystal structure of the nano-ZrO2 compound corresponds to the monoclinic symmetry P121/c1 - phase group (my research). The coefficient parameters are: a=5.1481 Å, b= 5.1962 Å, c=5.3132 Å, β=99.25°, Z=4, which corresponds to the results obtained during previous structural studies [9-21]. Calcination products of CS-ZrOx and PVA-ZrOx at 450, 800 and 1100 °C were subjected to X-ray difractmetry in order to determine crystallite phase composition and average size, and results obtained are shown in (Figure 10) (a and b). Te difractogram obtained for the 450 °C calcination product of CS-ZrOx (Figure 10a) displays broad difraction peaks at 2θ=30.3, 35.14, 50.48 and 60.2°, which match closely those fled for c-ZrO2 in JCPDS 27–099733,43. Te difractogram obtained for the calcination product at 800 °C (Figure 10a) exhibits a difraction pattern that may look generally similar to that displayed in the previous one, but

it is distinct by monitoring detectably sharper peaks and resolves fne structures near 2θ=35 and 60°. According to JCPDS 80–096533, these modifcations are diagnostic to formation of larger crystallites of t-ZrO2. On the other hand, the difractogram obtained for the calcination product of CS-ZrOx at the higher temperature of 1100 °C is shown (Figure 10a) to maintain similar, though narrower, peaks due to larger crystallites of t-ZrO_2, and to monitor, furthermore, new peaks at 2θ=28.2 and 31.4° that are quite indicative for formation of m-ZrO_2 crystallites (as per JCPDS 37–1484)33. Te derived average crystallite sizes allocate the smallest value (5.0nm) to c-ZrO_2, and the relatively largest value (20.3nm) to m-ZrO_2, whereas t-ZrO_2 is shown to exist in crystallites of intermediate sizes (8.1–16.2nm). These results are consitent with the size dependency limits of stability of each of three phases. Earlier reports focusing on the size dependence of structural stability in ZrO_2 particles, make clear that for nano-sized particles (where the surface/size ratio is high) the surface free energy has the upper hand in stabilizing the otherwise unstable c-ZrO_2 at low temperature, particularly in the absence of foreign ion dopants as in the present case.

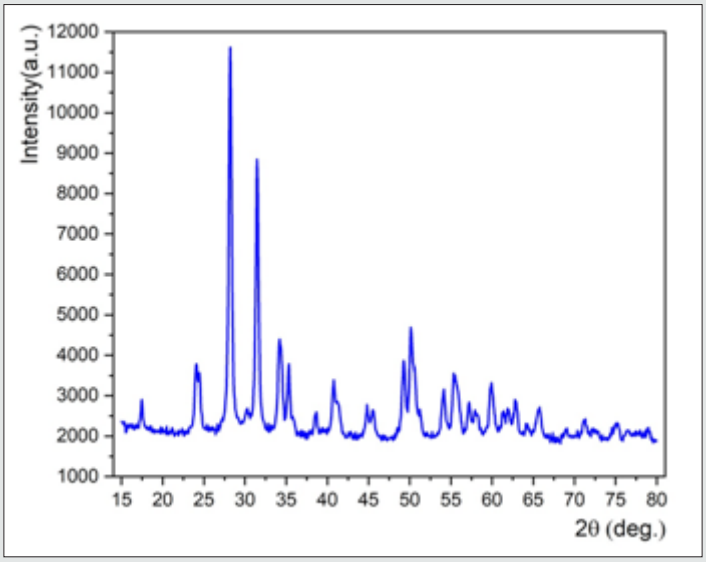

Figure 9: X-ray diffraction spectrum of the nano-ZrO_2 compound taken at the room temperature and in normal conditions.

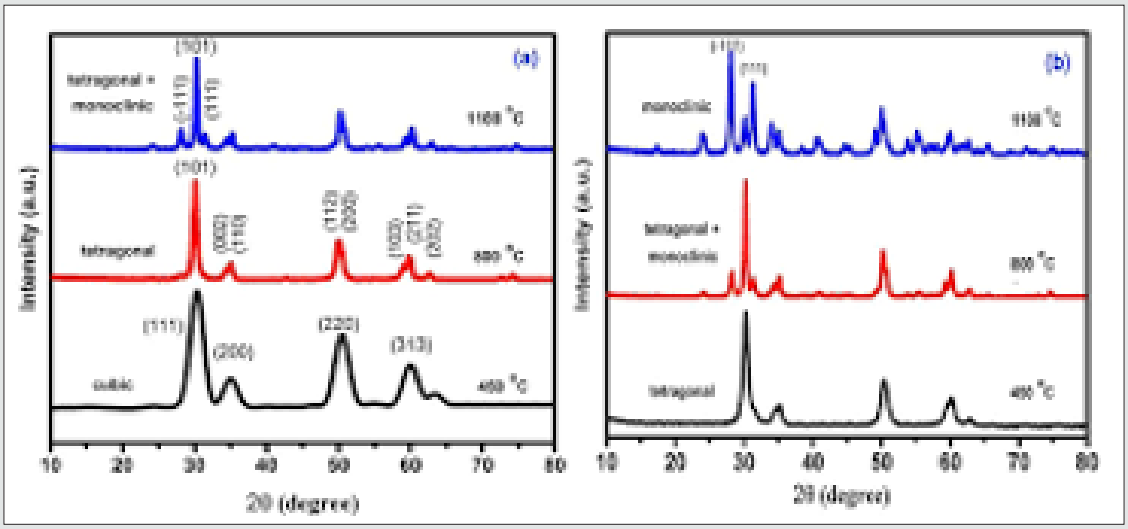

Figure 10: X-ray powder difractograms obtained for calcination products of CS-ZrOx (a) and PVA-ZrOx (b) hybrid flms at the temperatures indicated.

(Figure 10b) stacks X-ray difractograms obtained for calcination products of PVA-ZrOx. Te difraction pattern recorded for calcination product at 450°C is similar to that of the CS-ZrOx calcination product at 800°C (Figure 10a) in assigning the formation of t-ZrO_2. Whereas that obtained for the calcination product of PVA-ZrOx at 800 °C (Figure 10b) is similar to the pattern given rise by the calcination product of CS-ZrOx at the higher temperature of 1100 °C (Figure 10a) in accounting for formation of mixed t-/m-ZrO_2. Hence calcination of PVA-ZrOx at the the higher temperature of 1100 °C is found (Figure 10b) to advance the transformation of t-ZrO_2 into m-ZrO_2, which is the sole detectable crystallite phase for the zirconia nanoparticles thus recovered. It is obvious, that the average crystallite sizes determined for PVA-ZrOx calcination products at 450 (7.5nm), 800 (15.8nm) and 1100°C (29.2nm) may account for the failture in sustaining c-ZrO2 phase at 450°C (size >5nm), as well as for the instability of t-ZrO_2 in favour of m-ZrO_2 at 1100 °C (crystallite size approaching 30nm). Tese fndings suggest convincingly that the average crystallite size and, hence, the relative stability (or metastability) of the three crystallite phases of the recovered zirconia NPs are dependent not only on the thermal recovery conditions applied, but also on the polymer used in the hybrid flm [10].

The developed composite material was examined under Scanning Electron Microscope to find the formation of ZrO_2 particles and their surface morphology. X-diffraction test was carried out to confirm the formation of ZrO_2 phase's using D/MAX ULTIMA III XRD machine supplied by Rigaku Corporation (Rigaku-mini flex 600). X-ray diffraction pattern was obtained for the specimen using Cu kα radiation. The data were collected over the 2 Θ for the range of 10˚ to 120˚ degree with a step size of 0.02˚ degree and the scan speed of 10 degree/min. The X-ray diffraction pattern is well matched with the standard JCPDS (01-1176) of aluminium with a cubic crystal structure and Fm-3m space group. The absence of any additional peak other than aluminium in all the samples, confirms that the phase is the pure formation and no chemical reactions happen during casting process as shown in (Figure 11) [11]. The structural characterization of this nanocomposite (Figure 12) divulge that there is transition of crystal structure of ZrO2 from its pristine monoclinic to deviated monoclinic arrangement with increased unit cell volume of 163 Å3 . The high resolution TEM and SEM studies reveal that the ZrO2 is present in and around the nanotubes resulting in deviated monoclinic crystalline arrangement having crystallite size of 28.63 nm. The change in the crystalline structure provides increased surface area to immobilize the biomolecules required for the fabrication of an effective biosensor [12].

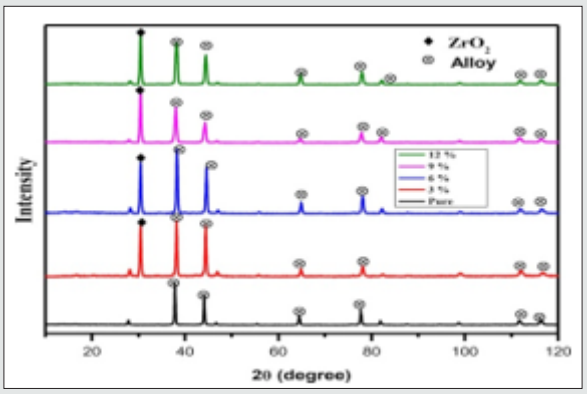

Figure 11: X-ray diffraction patterns of the specimen for LM25 with various wt% reinforcement of ZrO_2.

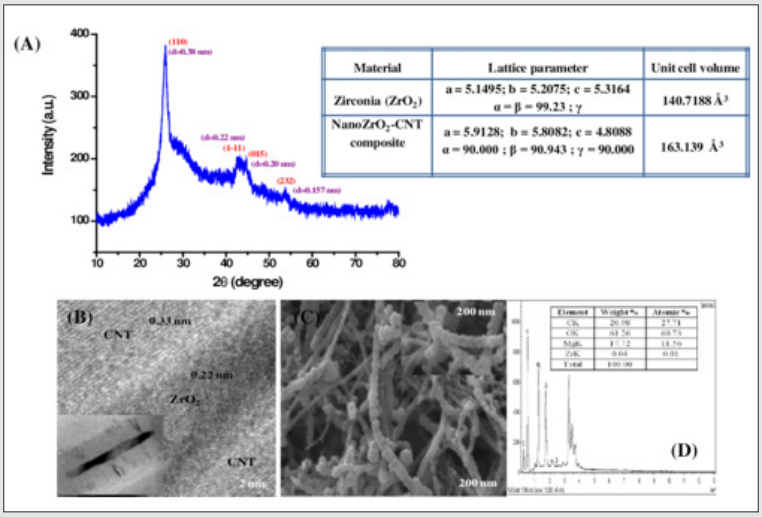

Figure 12: (A) XRD; (B) TEM ; (C) SEM and (D) EDX pattern of NanoZrO_2-CNT composite.

Conclusions

The X-ray diffraction spectrum by the Ritveld method revealed that the crystal structure of the nano-ZrO2 compound corresponds to the monoclinic symmetry P121/c1 - phase group. In this study, ZrO2 catalysts were synthesized by simple precipitation method and calcined at various temperatures. All samples showed pure tetragonal phase, except for ZrO2 (950) and ZrO2 (1000) catalysts that exhibited a mixture of tetragonal and monoclinic ZrO2 phases. The pure zirconia has three different crystal structures: monoclinic, m-ZrO2, tetragonal, t-ZrO2, and cubic, c-ZrO2.

References

1. Yong Han, Junfa Zhu (2013) Topics in Catalysis 56: 15-17.
2. Coloured Zirconia Ceramics (2018) J. Azo Nano November 15.
3. Masatomo Yashimaa and Shin Tsunekawab (2006) Structures and the oxygen deficiency of tetragonal and monoclinic zirconium oxide nanoparticles. Acta Cryst B62: 161-164.
4. Mohammed M Gad, Reem Abualsaud, Ahmed Rahoma, Ahmad M Al-Thobity (2018) Effect of zirconium oxide nanoparticles addition on the optical and tensile properties of polymethyl methacrylate denture base material. International Journal of Nanomedicine 13: 283-292.
5. Ghislaine Bertrand, et al. (2006) Structural and electronic properties of zirconia phases: A FP-LAPW investigations. Materials Science in Semiconductor Processing 9(6): 1006-1013.
6. Wikipedia, the free encyclopedia, Zirconium dioxide.
7. Zirconium dioxide, Practical Electron Microscopy and Database, Book.
8. Fan Qunbo, Wang Fuchi, Zhang Huiling and Zhang Feng (2008) Study of ZrO2 phase structure and electronic properties. Molecular Simulation 34(10-15): 1099-1103.
9. Imanova GT, Agayev TN, Jabarov SH (2020) Modern Physics Letters B 2150050.
10. Ali Bumajdad, Ahmed Abdel Nazeer, Fakhreia Al Sagheer, Shamsun Nahar (2018) Scientific Reports.
11. Karthikeyan Govindan, Jinu GR, Kannaiyan M (2019) Prediction of specific wear rate for LM25/ZrO_2 composites using Levenberg–Marquardt backpropagation algorithm. Matéria (Rio J.) 24(3).
12. Malhotra BD, Maumita Das and Pratima R Solanki (2012) Journal of Physics: Conference Series 358 012007.
13. Ali I, Imanova GT, Garibov AA, Agayev TN, Jabarov SH, et al. (2021) Radiation Physics and Chemistry 183: 109431.
14. Imanova GT, Hasanov SH (2020) Observation the initial radiation to the surface of mixed nano catalyst on oxidation processes. International Journal of Scientific and Engineering Research, USA, 11(8): 869-873.
15. Agayev TN, Garibov AA, Imanova GT, Melikova SZ (2018) J. High Energy Chemistry 52(2): 145-151.
16. Garibov AA, Agayev TN, Imanova GT (2017) J. Nanotechnologies in Russia12:(5-6): 22-26.
17. Agayev TN, Imanova GT, Musayeva SHZ (2021) Russian Journal of Physical Chemistry A 95(2): 270-272.
18. Imanova GT (2020) Advanced Physical Research 2: 94-101.
19. Garibov AA, Agaev TN, Imanova GT, Melikova SZ (2014) High energy chemistry, 48: 239-245.
20. Imanova GT, Agaev TN, Garibov AA, Melikova SZ, Jabarov SH, et al. (2021) Kinetic Interaction of Hexan Conversion and Oxidation on the Surface of an Al2O3 Nanocatalyzer at Room Temperature under the Effect of Gamma Radiation. Journal of Molecular Structure 1241: 130651.
21. Imanova GT (2021) Modern Approaches on Material Science 4: 508-514.

DOI: 10.32474/MAMS.2021.05.000201